

## M Dwarf catalog of LAMOST general survey data release one

Yan-Xin Guo<sup>1,3</sup>, Zhen-Ping Yi<sup>2</sup>, A-Li Luo<sup>1</sup>, You-Fen Wang<sup>1</sup>, Yu Bai<sup>1,3</sup>,  
Hai-Feng Yang<sup>1,3,4</sup>, Yi-Han Song<sup>1</sup>, Jian-Jun Chen<sup>1</sup>, Xiao-Yan Chen<sup>1</sup>, Fang Zuo<sup>1</sup>,  
Bing Du<sup>1</sup>, Jian-Nan Zhang<sup>1</sup>, Yin-Bi Li<sup>1</sup>, Xiao Kong<sup>1</sup>, Meng-Xin Wang<sup>1</sup>, Yue Wu<sup>1</sup>,  
Ke-Fei Wu<sup>1</sup>, Yong-Heng Zhao<sup>1</sup>, Yong Zhang<sup>5</sup>, Yong-Hui Hou<sup>5</sup>, Yue-Fei Wang<sup>5</sup> and  
Ming Yang<sup>1</sup>

<sup>1</sup> Key Laboratory of Optical Astronomy, National Astronomical Observatories, Chinese Academy of Sciences, Beijing 100012, China; [yxguo@bao.ac.cn](mailto:yxguo@bao.ac.cn)

<sup>2</sup> School of Mechanical, Electrical & Information Engineering, Shandong University at Weihai, Weihai 264209, China

<sup>3</sup> University of Chinese Academy of Sciences, Beijing 100049, China

<sup>4</sup> School of Computer Science and Technology, Taiyuan University of Science and Technology, Taiyuan 030024, China

<sup>5</sup> Nanjing Institute of Astronomical Optics & Technology, National Astronomical Observatories, Chinese Academy of Sciences, Nanjing 210042, China

Received 2015 March 15; accepted 2015 May 22

**Abstract** We present a spectroscopic catalog of 93 619 M dwarfs from the first data release of the Large Sky Area Multi-Object Fiber Spectroscopic Telescope (LAMOST) general survey. During sample selection, M giant contamination was eliminated using 2MASS photometry and CaH/TiO molecular indices. For each spectrum, the spectral subtype and values are provided including radial velocity,  $H\alpha$  equivalent width, a series of prominent molecular band indices, and the metal-sensitive parameter  $\zeta$ , as well as distances and the space motions for high S/N objects. In addition,  $H\alpha$  emission lines are measured to examine the magnetic activity properties of M dwarfs and 7179 active ones are found. In particular, a subsample with significant variation in magnetic activity is revealed through observations from different epochs. Finally, statistical analysis for this sample is performed, including the metallicity classification, the distribution of molecular band indices and their errors.

**Key words:** catalogs — methods: analytical — stars: statistical — stars : late-type — stars: magnetic-activity — stars

### 1 INTRODUCTION

Very cool, low-mass stars with late spectral types (M dwarfs) are the most abundant stars in the Galaxy and in the vicinity of the Sun (Reid & Cruz 2002; West et al. 2004), with a recent accounting indicating that M dwarfs outnumber higher mass stars by a factor of  $\sim 3$  (Lépine & Gaidos 2011).

Their main-sequence lifetimes are considerably greater than the Hubble time (Laughlin et al. 1997), and the metallicity variations have a significant effect on their spectral energy distribution (Allard & Hauschildt 1995). Therefore, they can not only serve as useful probes of star formation history in the local solar neighborhood (Gizis et al. 2002), but can also be used to trace the structure and evolution of the Milky Way. Previous studies elucidated the essential properties of low-mass stars (Hawley et al. 2002; West et al. 2004, 2005; Bochanski et al. 2007; Schmidt et al. 2010), Galactic kinematics (Hawley et al. 1996; Lépine et al. 2003; Bochanski et al. 2005, 2007, 2010), the stellar initial mass function (Covey et al. 2008; Bochanski et al. 2010), the structure of the local Milky Way's thin and thick disks (Reid et al. 1997; Kerber et al. 2001; Woolf & West 2012; Bochanski et al. 2013, 2014; Jurić et al. 2008; Fuchs et al. 2009), and potential habitable extrasolar planets around low-mass stars (Charbonneau et al. 2009; Vogt et al. 2010; Bean et al. 2010; Mann et al. 2011; Apps et al. 2010; Fischer et al. 2012).

With progress from wide-field, deep astronomical surveys (e.g., the Large Sky Area Multi-Object Fiber Spectroscopic Telescope (LAMOST), Sloan Digital Sky Survey (SDSS), Two Micron All Sky Survey (2MASS), 2dF and UKIRT Infrared Deep Sky Survey (UKIDSS)), a large amount of M dwarf spectra has been compiled. Consequently, many researches based on spectroscopic measurements of fundamental parameters have also made great progress, involving spectral subtype classification (Kirkpatrick et al. 1991, 1999; Reid et al. 1995a; Martín 1999; Reid & Cruz 2002; Hawley et al. 2002), radial velocity (RV) evaluation (Bochanski et al. 2007; West et al. 2011), metallicity estimation (Gizis 1997; Lépine et al. 2003, 2007, 2013; Woolf & Wallerstein 2006; Dhital et al. 2012), as well as tracking magnetic activity and flaring properties (Reid et al. 1995b; Hawley et al. 1996; Gizis et al. 2000, 2002; West et al. 2004, 2008, 2011; West & Hawley 2008; Kowalski et al. 2009; Kruse et al. 2010; Hilton et al. 2010).

LAMOST (also known as the Guo Shou Jing Telescope) carried out a pilot survey from 2011 October to 2012 June and obtained 319 000 spectra (Cui et al. 2012; Zhao et al. 2012; Luo et al. 2012). In the LAMOST pilot survey data release, about 58 360 M dwarfs were identified (Yi et al. 2014), accounting for 7% of all data released. Yi et al. (2014) ignored the giant contamination due to the low rate of giants, then described the methods adopted to derive fundamental parameters and verified their precision. The general survey has operated since 2012 September and has already released over 2 million spectra up to 2013 June (Luo et al. 2015). In the LAMOST general survey data release one, the number of M dwarfs will dramatically increase accordingly. In this paper, we will present a purer sample of M dwarfs from LAMOST Data Release 1 (DR1; Luo et al. 2015). Section 2 describes the data and sample purification techniques, which eliminates giants. The methods adopted to measure the fundamental parameters are illustrated in Section 3. In Section 4, we describe the general characteristics of the results, assess the uncertainty of molecular band indices, and examine the magnetic activity properties of M dwarfs, followed by an analysis of metallicity classification. Section 4 also contains a list of M dwarfs with significant variation in magnetic activity through observations that were taken in different epochs.

## 2 DATA AND SAMPLE SELECTION

### 2.1 LAMOST Survey Data

The LAMOST DR1 catalog contains more than 2 million spectra, including 710 000 spectra observed during the pilot survey which were reprocessed by the revised spectral reduction and analysis pipelines. After applying the LAMOST one-dimensional (1D) pipeline (Luo et al. 2004, 2015), a visual confirmation (Guo et al. 2012) is conducted to obtain the initial classifications of stars. Only the F, G and K type stellar spectra which meet the specific signal-to-noise (S/N) ratio criterion were input into the LAMOST stellar parameter pipeline (Luo et al. 2015; Wu et al. 2011) to derive stellar atmosphere parameters including  $T_{\text{eff}}$ ,  $\log g$ , Fe/H, RV and corresponding errors. During the visual inspection, we identified all M type spectra using the modified Hammer spectral typing facility (Yi

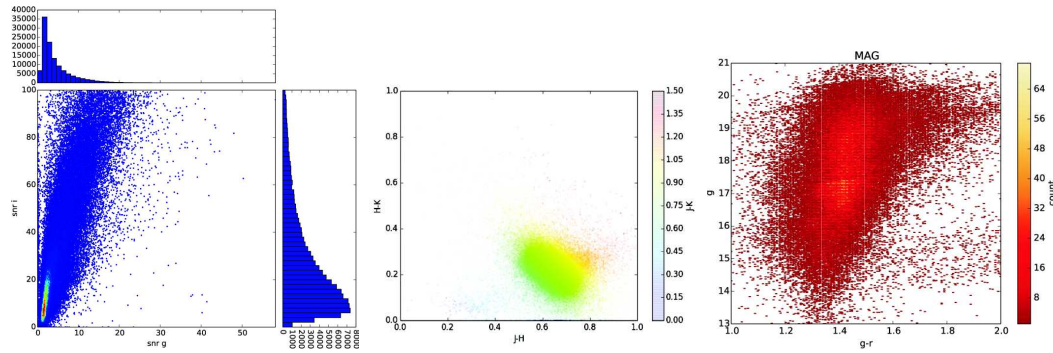


**Fig. 1** The left panel shows the S/N distribution of M type stars. The  $X$  axis denotes the S/N of the  $g$  band, the  $Y$  axis denotes the S/N of the  $i$  band, and the top and right subpanels show bar plots of S/N for each magnitude bin. The  $i$  band is obviously better than the  $g$  band. The middle panel shows the 2MASS color-color distribution. The right panel shows the  $g$  versus  $g - r$  Hess diagram. The colors denote the count at the corresponding position.

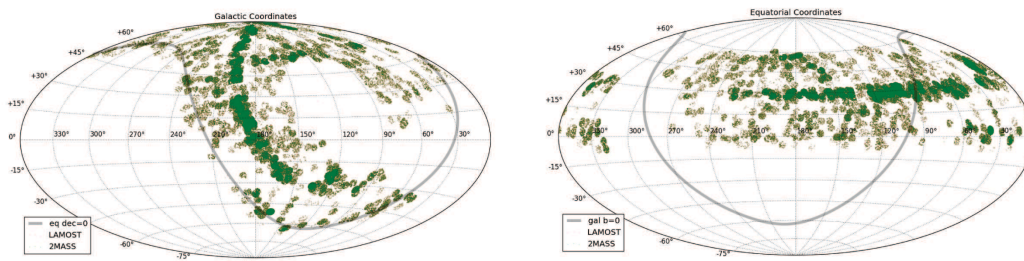


**Fig. 2** The Galactic coordinates and equatorial coordinates of all M type stars in LAMOST DR1 (in red) and the corresponding 2MASS objects (in green). The yellow ones mainly indicate where the cross-matched objects overlap.

et al. 2014; Covey et al. 2007). Regardless of S/N, we obtained 121 522 M type spectra of 103 467 different objects.

The entire spectral coverage is 3690 – 9100 Å, including a blue portion spanning the wavelength range of 3690 – 5900 Å and a red portion in the range 5700 – 9100 Å, with an overlap of about  $\sim 200$  Å. The S/N for bands  $g$  and  $i$  in Figure 1 shows that the red side of the spectra has higher quality. This is beneficial for tracking features in the red side of the spectrum of M dwarfs. Figure 1 also shows the  $g$  versus  $g - r$  Hess diagram for M type stars in LAMOST DR1, as well as the 2MASS color-color distribution.

## 2.2 2MASS Photometry

As an auxiliary means to eliminate giant contamination (see Sect. 2.3), infrared photometric information is indispensable. We cross-matched the 2MASS All-Sky Point Source Catalog for the  $JHK_s$  band magnitudes and found 121 536 counterpart objects within a  $5''$  search radius. Figure 2 shows the Galactic coordinates and equatorial coordinates for all M type stars in LAMOST DR1 and corresponding 2MASS objects.

### 2.3 Eliminating Giant Contamination

There are many previous works on M giants. Rocha-Pinto et al. (2003) selected M giants from 2MASS to trace the Galactic Anticenter stellar stream, and Bochanski et al. (2014) searched for M giants in the Galactic halo. There are two primary approaches to distinguish M giants from dwarfs. The first method uses spectral features, which depend on accurate spectrophotometric calibration and spectral quality. Compared to M dwarfs, M giants have weak NaI, KI, CaH and FeH (Gray & Corbally 2009; Schlieder et al. 2012). The CaII triplet, Fe/H and neutral Na in the near infrared band spectrum, as well as the CO molecular band in the  $H$  and  $K$  bands can also be used to separate giants from dwarfs (Cushing et al. 2005). Gizis (1997) and West et al. (2004) used the varying strengths of TiO5 and CaH molecular bands to define divisions between giants, dwarfs and subdwarfs. These features, if not obvious, may be hidden by noise so that the measurement will not be sufficiently accurate. Another alternative way is to use photometry and proper motion to identify giants or dwarfs. Bessell & Brett (1988) found that M giants and M dwarfs separate in  $J - H$  versus  $J - K$  color space due to differences in H<sub>2</sub>O absorption in their atmospheres. Yet using this criterion alone will introduce some QSO contamination. Phan-Bao et al. (2003) used a combination of reduced proper motion (Jones 1972) and color to separate M giants from M dwarfs.

Our determination of luminosity class combines both spectral features and 2MASS near-infrared photometry. On one hand, we use several gravity-sensitive molecular indices to identify possible M giants. Molecular indices are the ratios of the average flux levels in a specified wavelength region to those in a pseudo-continuum region. They are useful for M dwarfs where the continuum is poorly defined. Metal hydride bands, such as the CaH bands defined by Reid et al. (1995a) and Lépine et al. (2007) have been used for luminosity classification, although they are less useful for stars earlier than K7. We compare CaH1 and CaH3 indices to the TiO5 index, which we find are more sensitive than CaH2 for isolating M giants from M dwarfs. By applying this procedure, we derive 10 795 M giant spectra.

Figure 3 shows the distribution of CaH1 versus TiO5 molecular indices and CaH3 versus TiO5 molecular indices. The two branches in this diagram clearly indicate two distinct populations. As for spectral features, we follow Bessell & Brett (1988) to select objects meeting the criterion of  $J - H > 0.8$  and  $J - K > 1$  to find 5036 possible M giants spectra, which are mostly confirmed to be the same objects identified by spectral features.

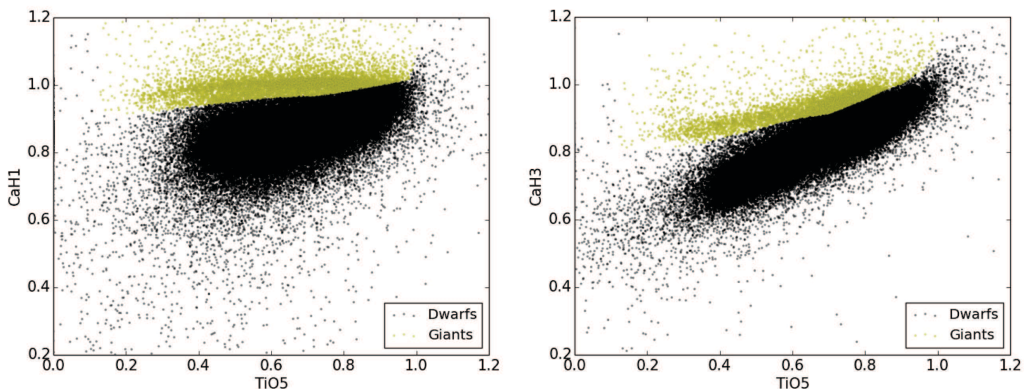


**Fig. 3** Distribution of CaH1 versus TiO5 molecular band indices and CaH3 versus TiO5 molecular band indices. Yellow dots indicate M giants.

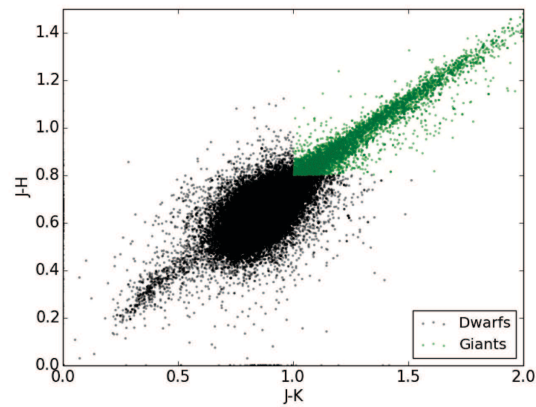


**Fig. 4**  $J-H$  vs.  $J-K$  color distribution for all M type stars in LAMOST DR1. The points shown in green indicate the M giants that we identified while the ones shown in black represent M dwarfs.

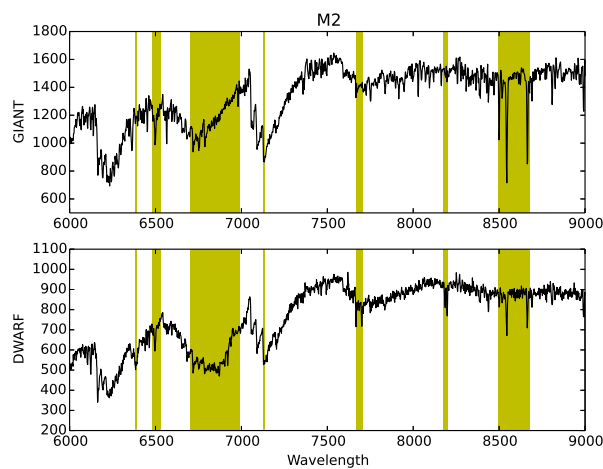


**Fig. 5** LAMOST spectra of an M dwarf (*bottom*) compared to an M giant (*top*) of the same subtype M2. Approximate regions for each of the seven indices used in giant/dwarf discrimination are highlighted in green. B1 refers to a mix of atomic lines (defined by West et al. 2011). Most notable in the giant spectra is the weakness in line strengths for the K I (7630 Å) and Na I doublets (8189 Å). Also weaker in the giants are the band strengths of CaH molecular bands and the ratio of indices between TiO5 (7125 – 7135 Å) and CaH. The CaH1 (6380 – 6390 Å) becomes stronger from M giants to M dwarfs and M subdwarfs. CaH2 (6814 – 6846 Å) and CaH3 (6960 – 6990 Å) have the same characteristics. Indeed, the Ca II triplet (8484 – 8662 Å) is relatively weak in the dwarf spectrum but it is quite strong in that from the giant.

Figure 4 shows  $J - H$  versus  $J - K$  color for all M type stars. M giants and M dwarfs are apparently separated. Combining these two results, we finally obtain 12 355 M giant spectra. After excluding these M giant candidates, we derive 110 321 M dwarf spectra of 93 619 distinct objects.

We show spectra of a giant star and a dwarf star with the same subtype in Figure 5, with the location of each feature highlighted. As can be seen, most atomic lines are stronger in dwarfs than in giants. The K I (7630 Å) and Na I doublets (8189 Å) are quite shallow in giants but relatively deep

in dwarfs. Also weaker in the giants are the band strengths of CaH molecular bands and the ratio of indices between TiO5 (7125 – 7135 Å) and CaH. The CaH1 (6380 – 6390 Å) becomes stronger from M giants to M dwarfs and M subdwarfs. CaH2 (6814 – 6846 Å) and CaH3 (6960 – 6990 Å) have the same characteristics. Indeed, the Ca II triplet (8484 – 8662 Å) emits comparatively more in dwarfs than in giants.

### 3 METHODS

We use the modified Hammer spectral typing facility (Yi et al. 2014; Covey et al. 2007) to process the LAMOST M dwarf spectra identified in Section 2.3. The prominent features, including 16 atomic lines (Ca II, Na I, Rb and Cs) and molecular lines (CaH, TiO, VO and CrH) as well as one color (Color6545; Yi et al. 2014) are calculated to estimate the spectral type.

Tables 1 and 2 summarize the wavelength boundaries and weights of each index above.

**Table 1** Single Numerator of Modified Hammer Spectral Indices

Spectral Feature	$\lambda_w$ (Å)	$\lambda_{cont}$ (Å)
CaH6385	6385	6389
Color6545	6545	6549
CaH3	6960	6990
TiO5	7126	7135
VO7434	7430	7470
VO7912	7900	7980
NaI8189	8177	8201
TiO8250	8250	8254
TiO B	8400	8415
TiO8440	8440	8470
CaII8498	8483	8513
CrH-a	8580	8600

**Table 2** Multiple Numerators of Modified Hammer Spectral Indices

Spectral Feature	$\lambda_{w1}$ (Å)	weight1	$\lambda_{w2}$ (Å)	weight2	$\lambda_{cont}$ (Å)
VO-a	7350	7400	0.56	7510	7560
VO-b	7860	7880	0.5	8080	8100
Rb-b	6960	6990	0.5	7962.6	7972.6
Cs-a	7126	7135	0.5	8536.1	8546.1

The RV of each M dwarf is measured by the cross-correlation method (Yi et al. 2014). Each observed spectrum is cross-correlated with the Bochanski et al. (2007) M dwarf template of the best matching subtype. The precision of this method is verified by Yi et al. (2014).

The H $\alpha$  emission line is the strongest and best-studied indicator of chromospheric magnetic activity in late-type stars (in contrast to solar-type stars, which are usually traced by Ca II H and K resonance lines). We examine the magnetic activity properties of M dwarfs following a method similar to Yi et al. (2014) and West et al. (2004, 2011). An active M dwarf needs to satisfy the following four criteria.

- (1) The S/N (H $\alpha$  S/N) of the continuum near H $\alpha$  must be larger than 3.
- (2) The equivalent width (EW) of the H $\alpha$  line must be larger than 1.
- (3) The EW of the H $\alpha$  line is larger than three times its error.
- (4) The height of the H $\alpha$  emission line is larger than three times the noise in the adjacent continuum.

We measure the molecular band features (TiO1-5, CaH1-3, CaOH) following Reid et al. (1995a). In addition, the metallicity-sensitive indicator  $\zeta$  is calculated to roughly discern the metallicity type: dwarf (dM), subdwarf (sdM), extreme dwarf (esdM) and ultra subdwarf (usdM) (Lépine et al. 2007, 2013).

## 4 RESULTS AND DISCUSSION

### 4.1 Spectral Types

As mentioned in Section 2.1, all of the LAMOST M dwarfs processed by the modified Hammer spectral typing facility were individually visually checked to select more accurate subtypes, although only a very small fraction of these spectra were misclassified within one subtype. Figure 6 shows the distribution of spectral subtypes of M dwarfs in LAMOST DR1.

### 4.2 RV

Using our RV results, all M dwarf spectra are corrected to their rest frame wavelength by measuring their  $H\alpha$  emission line and the molecular band indices. Figure 7 shows the RV distribution of M dwarfs in LAMOST DR1.

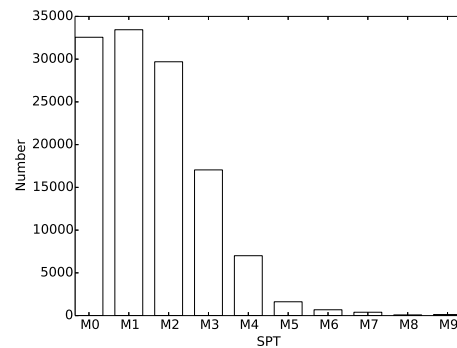


**Fig. 6** Distribution of spectral subtypes of M dwarfs in LAMOST DR1.

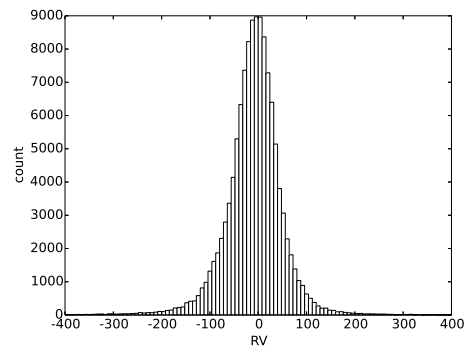


**Fig. 7** RV distribution of M dwarfs in LAMOST DR1.

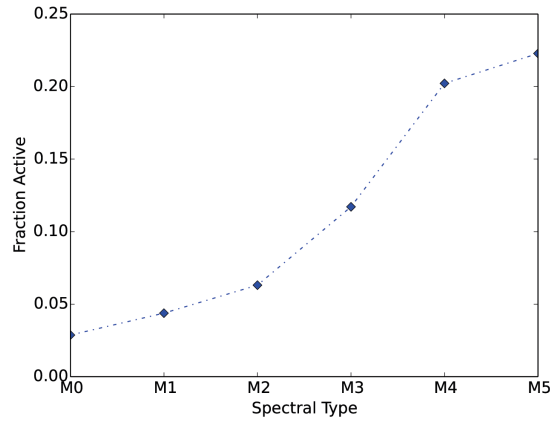


**Fig. 8** H $\alpha$  magnetic activity fraction versus spectral type. The fractions for M6-M9 are ignored due to their small size in the sample. The fractions for M0-M5 show a rising trend consistent with existing literatures.

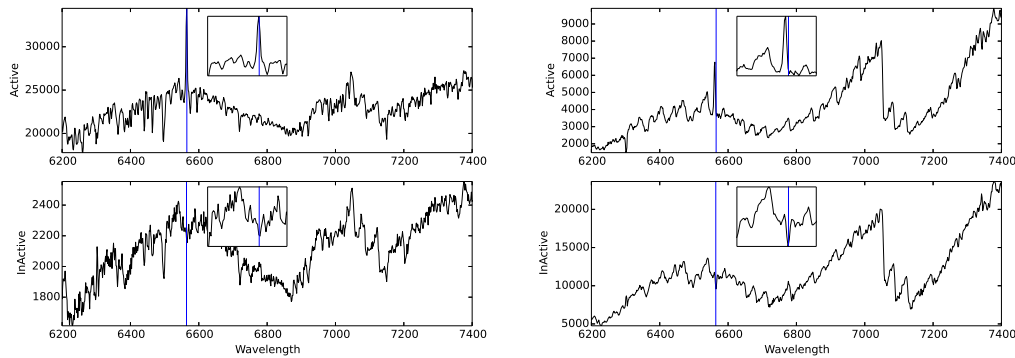


**Fig. 9** Comparison of spectra for both active and inactive cases for M0 (*left*) and M4 (*right*) stars. Wavelength ranges from 6200 Å to 7400 Å. Small boxes in each panel contain a section of the spectrum near H $\alpha$ . The solid lines label the wavelength of H $\alpha$ .

### 4.3 Magnetic Activity

Using the magnetic activity criteria mentioned in Section 3, 7179 of 110 321 M dwarf spectra are active while 43 268 are inactive, and a portion of spectra cannot be precisely determined due to their poor S/N. Figure 8 shows the trend in the fraction of active stars from M0 to M5. The fractions of H $\alpha$  activity for each spectral type are also listed in Table 3. We ignore M6-M9 because of their small number in our sample. Our results are consistent with previous studies that show H $\alpha$  emission increases from early to mid M spectral types (Joy & Abt 1974; Hawley et al. 1996; West et al. 2011).

Figure 9 shows examples of both active and inactive spectra for M0 and M4 subtypes. The continuum features near H $\alpha$  are noticeable in the inactive stars, but it is clear that no measurable emission at H $\alpha$  is present. However, active stars have a clearly measurable H $\alpha$  feature. Moreover, we use 2MASS near-infrared photometry ( $JHK_s$ ) to investigate the photometric properties of active stars. Figure 10 shows that 2MASS colors of active M dwarfs are very similar to those of the

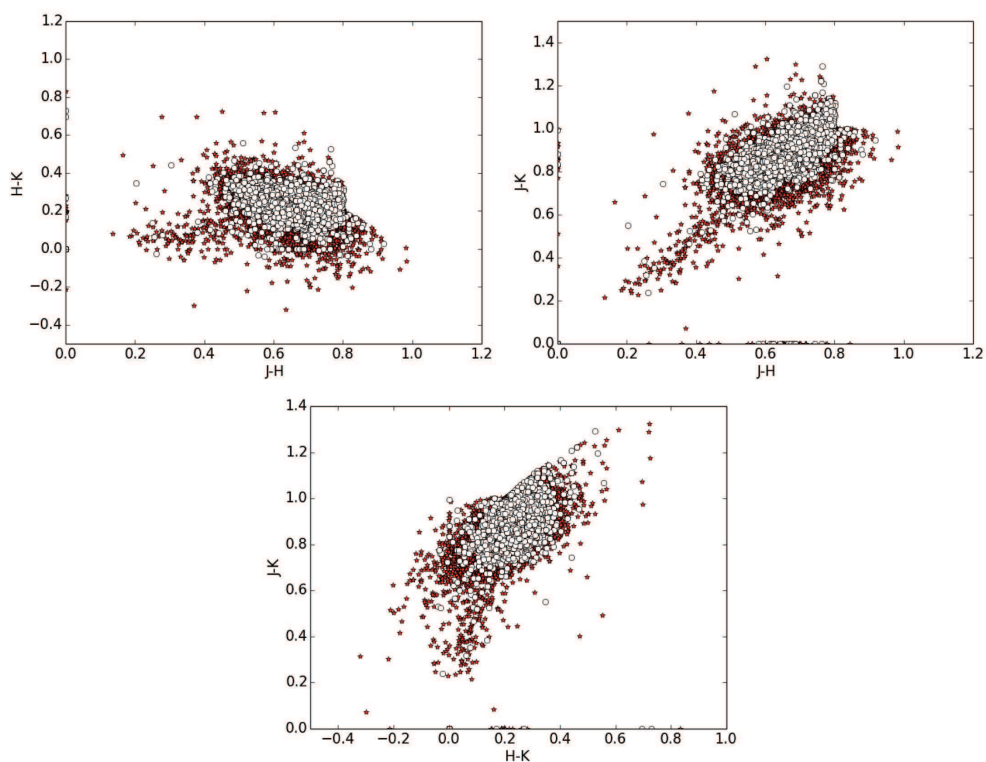


**Fig. 10** Three color-color diagrams in 2MASS  $JHK_s$  are used to compare colors of active dwarfs (*hollow circles*) to inactive dwarfs (*red stars*). There is no significant difference between active and inactive dwarfs in any combination of the colors.

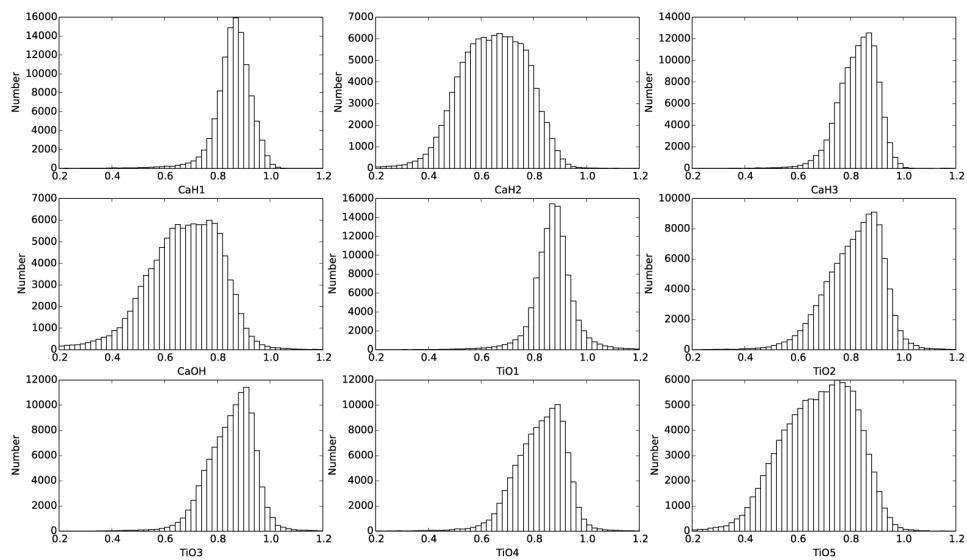


**Fig. 11** Distribution of each molecular band index. From left to right, and top to bottom, the distributions of CaH1, CaH2, CaH3, CaOH, TiO1, TiO2, TiO3, TiO4 and TiO5 are shown respectively.

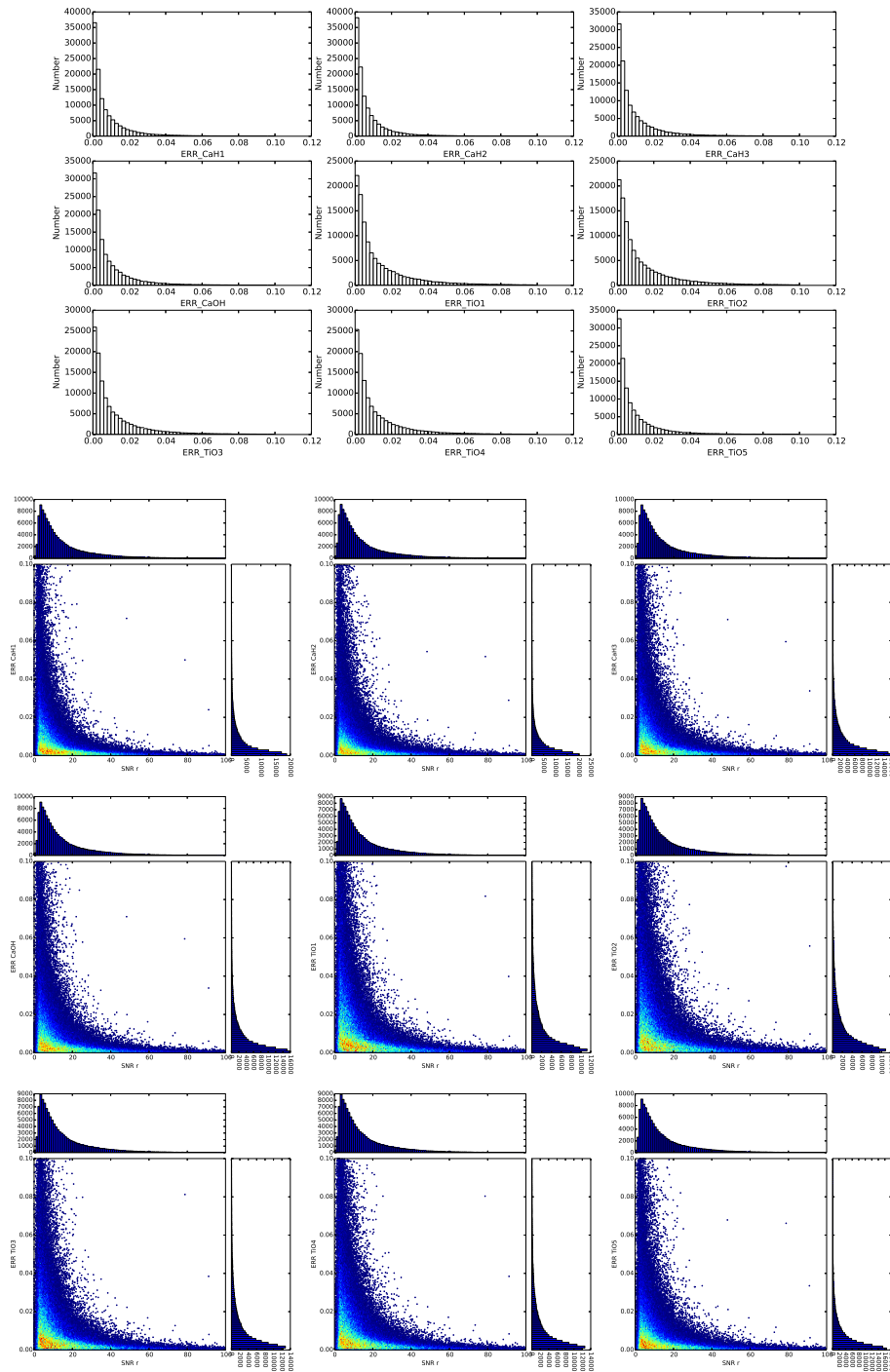


**Fig. 12** Error distribution of each molecular band index. The top nine distributions are in the same order as Fig. 11. The bottom nine distributions show a decreasing trend in error with an increase in S/N. The order for the bottom nine distributions is also the same as in Fig. 11.

**Table 3** H $\alpha$  Magnetic Activity Fraction for Each Subtype

Subtype	Total	Active	Active Fraction	Inactive	Inactive Fraction	Ambiguous
M0	30339	871	0.0287	19174	0.6320	0.3493
M1	30257	1324	0.0438	13083	0.4324	0.5338
M2	26674	1687	0.0632	7481	0.2805	0.6663
M3	15301	1800	0.1176	2856	0.1867	0.7057
M4	5876	1187	0.2020	636	0.1082	0.6998
M5	1212	271	0.2236	30	0.0248	0.7616

**Table 4** Objects with Significant Variation in Magnetic Activity during Different Observations

Designation	RA	Dec	Subtype	obsdate1	act1	obsdate2	act2	obsdate3	act3
J005728.33+374156.4	14.368071	37.699	M1	2011-11-08	i	2011-12-12	a	...	...
J005827.91+375909.3	14.616319	37.985935	M3	2011-11-08	a	2012-10-07	i	...	...
J014426.41+280728.1	26.110068	28.124488	M2	2012-01-04	a	2012-01-13	i	...	...
J023409.96+044926.0	38.5415	4.8238976	M1	2012-12-09	i	2013-01-08	a	...	...
J030659.20+271432.8	46.746668	27.242467	M0	2012-01-12	i	2013-02-08	a	...	...
J033112.45+264923.3	52.801877	26.823162	M3	2012-10-05	a	2013-02-07	i	...	...
J040207.95+282915.1	60.533138	28.48755	M1	2011-12-18	a	2012-01-23	i	...	...
J044302.44+234423.0	70.760184	23.739737	M2	2012-12-23	a	2012-12-31	i	...	...
J051309.63+290313.9	78.290165	29.053867	M2	2011-12-14	i	2013-02-15	a	...	...
J051516.65+263739.5	78.819394	26.627648	M2	2012-10-29	a	2013-03-05	i	...	...
J052251.61+303131.4	80.715044	30.525413	M2	2011-12-14	i	2012-10-07	a	...	...
J062510.93+275238.8	96.295551	27.877471	M1	2011-10-27	i	2011-11-08	a	...	...
J065243.79+283624.2	103.18246	28.606734	M1	2011-10-28	a	2011-11-09	i	...	...
J070619.78+280527.0	106.58243	28.090855	M3	2011-10-28	i	2011-12-14	a	2011-12-21	i
J070916.85+303248.0	107.32021	30.546672	M1	2011-12-27	i	2013-02-08	a	...	...
J071333.29+330656.3	108.38873	33.11566	M0	2012-11-07	a	2013-03-09	i	...	...
J071433.98+293455.7	108.6416	29.582166	M3	2011-11-23	i	2013-03-09	a	...	...
J073756.02+272018.9	114.48342	27.338584	M3	2011-11-10	a	2011-12-25	i	...	...
J090746.63+272223.3	136.944319	27.37314	M0	2011-11-11	i	2012-02-01	a	...	...
J110006.88+263130.8	165.028675	26.525248	M3	2011-12-14	a	2012-03-11	i	...	...
J110534.39+282540.4	166.393314	28.427891	M3	2011-12-14	a	2012-01-04	i	...	...
J114649.69+012518.1	176.707074	1.421704	M1	2012-12-22	a	2012-12-24	i	...	...
J120024.56+292310.3	180.102351	29.3862	M1	2012-01-12	a	2012-02-03	i	...	...
J121625.53+315051.2	184.106401	31.847574	M1	2012-01-03	a	2012-02-03	i	...	...
J122433.93+263428.1	186.141398	26.574497	M3	2011-11-08	a	2012-10-07	i	...	...

Notes: The labels obsdate1, obsdate2 and obsdate3 denote the different dates for observations. The labels act1, act2 and act3 denote magnetic activity measurements in observations from different epochs, and a and i indicate active and inactive cases respectively.

inactive ones. There is no significant relationship between magnetic activity properties and infrared photometry.

It is interesting that we confirmed 25 of 93 619 M dwarfs show significant variation in H $\alpha$  magnetic activity through different epochs when observations were acquired, active to inactive, inactive to active, or active at some times and inactive at the other times. This means these dwarfs were experiencing unstable magnetic activity. A description of the subsample with their magnetic activity properties is given in Table 4.

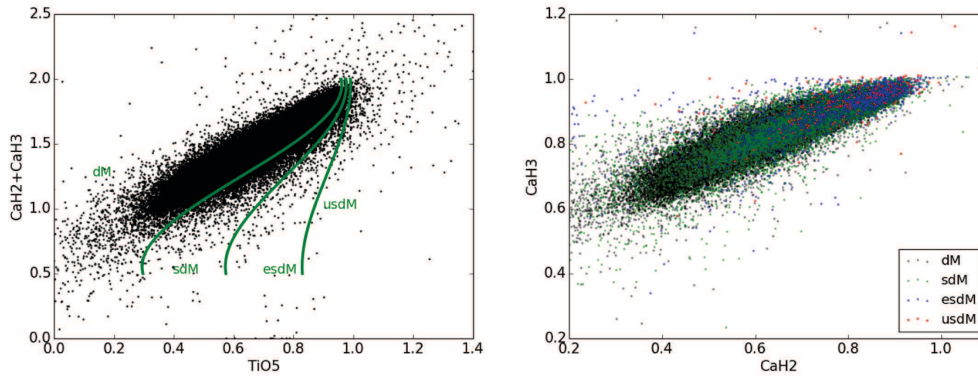


**Fig. 13** *Left:* Metallicity class distribution of M dwarfs in LAMOST DR1 based on the  $\text{CaH2} + \text{CaH3}/\text{TiO5}$  relationship. *Right:* distribution of the  $\text{CaH2}$  and  $\text{CaH3}$  spectral indices for M dwarfs and subdwarfs. This suggests that ultra subdwarfs are located in the upper-right part of the distribution.

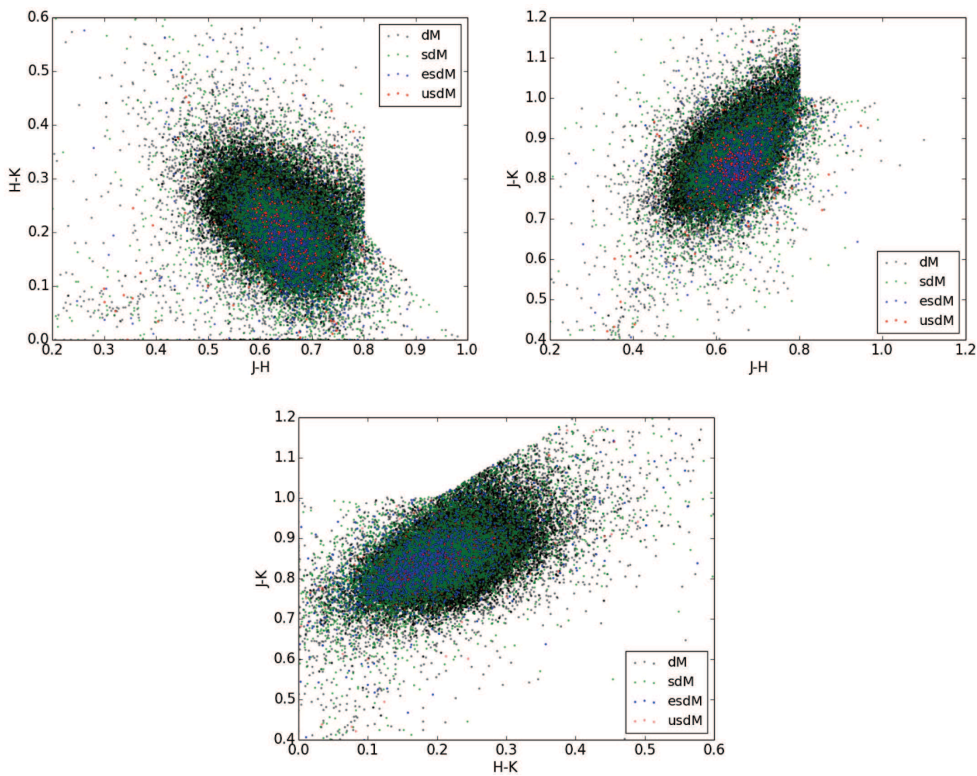


**Fig. 14** Several color-color diagrams in the 2MASS  $JHK_s$ . There are no significant differences among different metallicity classes in any of the colors.

#### 4.4 Molecular Band Indices

Nine important molecular band indices and their corresponding errors (as mentioned in Sect. 3) are measured. Figures 11 and 12 show the distribution of each feature and its error. Figure 12 suggests that as S/N increases the error becomes dramatically smaller.

#### 4.5 Metallicity Indicator

Metallicity is one of the most elusive physical quantities to measure in M dwarfs. We use the definition from Lépine et al. (2013) to measure the metallicity sensitive parameter  $\zeta$ , which is currently the best indicator of metallicity for optical M dwarf spectra. Metal poor M dwarfs can be classified into four metallicity categories by estimating the parameter  $\zeta_{\text{TiO}/\text{CaH}}$ : dM ( $\zeta > 0.825$ ), sdM ( $0.5 < \zeta < 0.825$ ), esdM ( $0.2 < \zeta < 0.5$ ), and usdM ( $\zeta < 0.2$ ).  $\zeta_{\text{TiO}/\text{CaH}}$  is formally defined as follows

$$\zeta = \frac{1 - \text{TiO5}}{1 - [\text{TiO5}]_Z}, \quad (1)$$

$$[\text{TiO5}]_Z = 0.622 - 1.906[\text{CaH}] + 2.211[\text{CaH}]^2 - 0.588[\text{CaH}]^3, \quad [\text{CaH}] = \text{CaH2} + \text{CaH3} \quad (2)$$

Figure 13 shows the distribution of spectral indices for M dwarfs in LAMOST DR1 and the rough separators for metallicity classification. In addition, the distribution of the CaH2 versus CaH3 indices is also given. It suggests that ultra subdwarfs are located in the upper-right of the distribution, which means CaH2 may be more sensitive to metallicity.

In order to explore any relationship between 2MASS photometry and metallicity classes, we examine each distribution of metallicity in the catalog with three color-color diagrams. The results are shown in Figure 14. However, it is suggested that there are no significant differences among different metallicity classes in any of the colors.

## 5 SUMMARY

We present a spectroscopic M dwarf catalog from LAMOST DR1, which consists of 110321 M dwarf spectra of 93619 objects. Our catalog not only includes the spectral subtypes, RVs, EWs of  $H\alpha$ , magnetic activity, nine molecular band indices and their errors, and metal-sensitive parameter  $\zeta$ , but also provides 2MASS photometric information. This catalog can be downloaded from the web site [http://paperdata.china-vo.org/Guoyx/2015/DR1\\_M\\_catalog.txt](http://paperdata.china-vo.org/Guoyx/2015/DR1_M_catalog.txt), and their distances and space motions ( $U$ ,  $V$ ,  $W$ ) are also available for high S/N objects. Using a sample of more than 120000 candidates from the LAMOST spectroscopic database, we combine the 2MASS infrared photometry and CaH/TiO5 ratio to eliminate possible M giant contamination. By examining the distributions of S/N, magnitude and spectral subtype, as well as RV, we gain an overall understanding of M dwarfs in LAMOST DR1. We also analyze some bulk attributes of our sample, including molecular band features, magnetic activity, metallicity features and their relationship with 2MASS photometry. With the above statistical results, it is helpful to further identify M giants to learn more about LAMOST M dwarfs. Data Release 2 (DR2, Liu et al. 2015) of the LAMOST general survey has been made available and contains over 4.1 million spectra, which will enlarge the sample of M dwarfs and facilitate more studies that explore the structure and evolution of the Milky Way in the future.

**Acknowledgements** This research is supported by the Major State Basic Research Development Program of China (973 Program, No. 2014CB845700) and the National Natural Science Foundation of China (Grant Nos. 11390371 and 11303061). This research has made use of LAMOST data. The Guo Shou Jing Telescope (the Large Sky Area Multi-Object Fiber Spectroscopic Telescope, LAMOST) is a National Major Scientific Project built by the Chinese Academy of Sciences. Funding

for the project has been provided by the National Development and Reform Commission. This research also makes use of data products from the Two Micron All Sky Survey, which is a joint project of the University of Massachusetts and the Infrared Processing and Analysis Center/California Institute of Technology, funded by the National Aeronautics and Space Administration and the National Science Foundation.

## References

- Allard, F., & Hauschildt, P. H. 1995, *ApJ*, 445, 433  
Apps, K., Clubb, K. I., Fischer, D. A., et al. 2010, *PASP*, 122, 156  
Bean, J. L., Seifahrt, A., Hartman, H., et al. 2010, *ApJ*, 713, 410  
Bessell, M. S., & Brett, J. M. 1988, *PASP*, 100, 1134  
Bochanski, J. J., Hawley, S. L., Reid, I. N., et al. 2005, *AJ*, 130, 1871  
Bochanski, J. J., Munn, J. A., Hawley, S. L., et al. 2007, *AJ*, 134, 2418  
Bochanski, J. J., Hawley, S. L., Covey, K. R., et al. 2010, *AJ*, 139, 2679  
Bochanski, J. J., Hawley, S. L., Covey, K. R., et al. 2013, *Astronomische Nachrichten*, 334, 44  
Bochanski, J. J., Willman, B., West, A. A., Strader, J., & Chomiuk, L. 2014, *AJ*, 147, 76  
Charbonneau, D., Berta, Z. K., Irwin, J., et al. 2009, *Nature*, 462, 891  
Covey, K. R., Ivezić, Ž., Schlegel, D., et al. 2007, *AJ*, 134, 2398  
Covey, K. R., Hawley, S. L., Bochanski, J. J., et al. 2008, *AJ*, 136, 1778  
Cui, X.-Q., Zhao, Y.-H., Chu, Y.-Q., et al. 2012, *RAA (Research in Astronomy and Astrophysics)*, 12, 1197  
Cushing, M. C., Rayner, J. T., & Vacca, W. D. 2005, *ApJ*, 623, 1115  
Dhital, S., West, A. A., Stassun, K. G., et al. 2012, *AJ*, 143, 67  
Fischer, D. A., Gaidos, E., Howard, A. W., et al. 2012, *ApJ*, 745, 21  
Fuchs, B., Dettbarn, C., Rix, H.-W., et al. 2009, *AJ*, 137, 4149  
Gizis, J. E. 1997, *AJ*, 113, 806  
Gizis, J. E., Monet, D. G., Reid, I. N., et al. 2000, *AJ*, 120, 1085  
Gizis, J. E., Reid, I. N., & Hawley, S. L. 2002, *AJ*, 123, 3356  
Gray, R. O., & Corbally, J. C. 2009, *Stellar Spectral Classification* (Princeton: Princeton Univ. Press)  
Guo, Y., Luo, A., Wang, F., Bai, Z., & Li, J. 2012, in *Society of Photo-Optical Instrumentation Engineers (SPIE) Conference Series*, 8451, 2  
Hawley, S. L., Gizis, J. E., & Reid, I. N. 1996, *AJ*, 112, 2799  
Hawley, S. L., Covey, K. R., Knapp, G. R., et al. 2002, *AJ*, 123, 3409  
Hilton, E. J., West, A. A., Hawley, S. L., & Kowalski, A. F. 2010, *AJ*, 140, 1402  
Jones, E. M. 1972, *ApJ*, 173, 671  
Joy, A. H., & Abt, H. A. 1974, *ApJS*, 28, 1  
Jurić, M., Ivezić, Ž., Brooks, A., et al. 2008, *ApJ*, 673, 864  
Kerber, L. O., Javiel, S. C., & Santiago, B. X. 2001, *A&A*, 365, 424  
Kirkpatrick, J. D., Henry, T. J., & McCarthy, Jr., D. W. 1991, *ApJS*, 77, 417  
Kirkpatrick, J. D., Reid, I. N., Liebert, J., et al. 1999, *ApJ*, 519, 802  
Kowalski, A. F., Hawley, S. L., Hilton, E. J., et al. 2009, *AJ*, 138, 633  
Kruse, E. A., Berger, E., Knapp, G. R., et al. 2010, *ApJ*, 722, 1352  
Laughlin, G., Bodenheimer, P., & Adams, F. C. 1997, *ApJ*, 482, 420  
Lépine, S., Rich, R. M., & Shara, M. M. 2003, *AJ*, 125, 1598  
Lépine, S., Rich, R. M., & Shara, M. M. 2007, *ApJ*, 669, 1235  
Lépine, S., & Gaidos, E. 2011, *AJ*, 142, 138  
Lépine, S., Hilton, E. J., Mann, A. W., et al. 2013, *AJ*, 145, 102  
Liu, X. W., Zhao, G., & Hou, J. L. 2015, *RAA (Research in Astronomy and Astrophysics)*, 15, 1089

- Luo, A.-L., Zhang, Y.-X., & Zhao, Y.-H. 2004, in Society of Photo-Optical Instrumentation Engineers (SPIE) Conference Series, 5496, Advanced Software, Control, and Communication Systems for Astronomy, eds. H. Lewis, & G. Raffi, 756
- Luo, A.-L., Zhang, H.-T., Zhao, Y.-H., et al. 2012, RAA (Research in Astronomy and Astrophysics), 12, 1243
- Luo, A.-L., Zhao, Y.-H., Zhao, G., et al. 2015, RAA (Research in Astronomy and Astrophysics), 15, 1095
- Mann, A. W., Gaidos, E., & Aldering, G. 2011, PASP, 123, 1273
- Martín, E. L. 1999, MNRAS, 302, 59
- Phan-Bao, N., Crifo, F., Delfosse, X., et al. 2003, A&A, 401, 959
- Reid, I. N., Hawley, S. L., & Gizis, J. E. 1995a, AJ, 110, 1838
- Reid, N., Hawley, S. L., & Mateo, M. 1995b, MNRAS, 272, 828
- Reid, I. N., Gizis, J. E., Cohen, J. G., et al. 1997, PASP, 109, 559
- Reid, I. N., & Cruz, K. L. 2002, AJ, 123, 2806
- Rocha-Pinto, H. J., Majewski, S. R., Skrutskie, M. F., & Crane, J. D. 2003, ApJ, 594, L115
- Schlieder, J. E., Lépine, S., Rice, E., et al. 2012, AJ, 143, 114
- Schmidt, S. J., West, A. A., Hawley, S. L., & Pineda, J. S. 2010, AJ, 139, 1808
- Vogt, S. S., Butler, R. P., Rivera, E. J., et al. 2010, ApJ, 723, 954
- West, A. A., Hawley, S. L., Walkowicz, L. M., et al. 2004, AJ, 128, 426
- West, A. A., Walkowicz, L. M., & Hawley, S. L. 2005, PASP, 117, 706
- West, A. A., & Hawley, S. L. 2008, PASP, 120, 1161
- West, A. A., Hawley, S. L., Bochanski, J. J., et al. 2008, AJ, 135, 785
- West, A. A., Morgan, D. P., Bochanski, J. J., et al. 2011, AJ, 141, 97
- Wolf, V. M., & Wallerstein, G. 2006, PASP, 118, 218
- Wolf, V. M., & West, A. A. 2012, MNRAS, 422, 1489
- Wu, Y., Luo, A.-L., Li, H.-N., et al. 2011, RAA (Research in Astronomy and Astrophysics), 11, 924
- Yi, Z., Luo, A., Song, Y., et al. 2014, AJ, 147, 33
- Yi, Z.-P., Luo, A.-L., Zhao, J.-K., et al. 2015, RAA (Research in Astronomy and Astrophysics), 15, 860
- Zhao, G., Zhao, Y.-H., Chu, Y.-Q., Jing, Y.-P., & Deng, L.-C. 2012, RAA (Research in Astronomy and Astrophysics), 12, 723